


Article

Optimization of the Technological Parameters for Obtaining Zn-Ti Based Composites to Increase the Performance of H₂S Removal from Syngas

Annette Madelene Dăncilă ¹, Simona Căprărescu ¹, Constantin Bobirică ¹, Violeta Purcar ², Gabriel Gârleanu ³ , Eugeniu Vasile ⁴, Cristina Modroga ^{1,*}, Claudia Borda ³ and Dan Dobrotă ^{5,*} 

¹ Faculty of Applied Chemistry and Materials Science, University POLITEHNICA of Bucharest, Polizu 1-7, RO-060042 Bucharest, Romania; annette.dancila@upb.ro (A.M.D.); simona.caprarescu@upb.ro (S.C.); constantin.bobirica@upb.ro (C.B.)

² National Research and Development Institute for Chemistry and Petrochemistry-ICECHIM, Splaiul Independentei 202, 060021 Bucharest, Romania; violeta.purcar@icechim.ro

³ Faculty of Industrial Engineering and Robotics, Politehnica University of Bucharest, 060042 Bucharest, Romania; gabriel.garleanu@upb.ro (G.G.); claudia.borda@upb.ro (C.B.)

⁴ Institute of Research and Development "METAV" SA, C.A. Rosetti 31, 020011 Bucharest, Romania; eugeniu.vasile@upb.ro

⁵ Faculty of Engineering, Lucian Blaga University of Sibiu, 550024 Sibiu, Romania

* Correspondence: cristina.modroga@upb.ro (C.M.); dan.dobrota@ulbsibiu.ro (D.D.); Tel.: +40-214-023-820 (C.M.); +40-0722-446-082 (D.D.)

Received: 7 April 2020; Accepted: 7 May 2020; Published: 10 May 2020



Abstract: The realization of some composite materials that allow the best removal of H₂S from syngas was the main objective of this work. Thus, the optimization of the technological parameters for obtaining composites based on Zn-Ti was achieved. The paper studies the influence of calcination temperature on the characteristics of the binary ZnO-TiO₂ system used to synthesize a composite material with suitable properties to be used subsequently for syngas treatment. The mineralogical and structural analyzes showed that starting with the calcination temperature of 700 °C the material synthesized is composed mainly of zinc orthotitanate which possess the corresponding characteristics to be finally used in the treatment of the syngas for its desulfurization. At this calcination temperature the material has a compact structure most likely due to sintering of the formed titanates. These composites have a texture that places them rather in the category of non-porous materials, the pore volume and their surface area obviously decreasing as the calcination temperature increases. A maximum sulfur removal degree of about 97% was obtained by using a composite synthesized at a temperature of 700 °C (ZT-700).

Keywords: technological parameters; composites; optimization; syngas; hydrogen sulfide

1. Introduction

Gasification of renewable carbonaceous resources is currently one of the most important worldwide energy resources, mainly due to their availability, low cost, and environmental benefits [1,2]. Carbonaceous biomass such as sugar and starch crops (i.e., sugar beet, grains and tubers), oil crops (i.e., palm, rapeseed, sunflower), lignocellulosic plants (i.e., willow and eucalyptus), lignocellulosic biomass residue-derived agroforestry industries, and algae biomass, represents over 70% of all renewable energy production, and up to 10% of the worldwide total energy supply [3]. Steam gasification or supercritical water gasification in conjunction with wide range of catalysts such as alkaline earth metallic

catalysts (i.e., NaOH, KOH, Na_2CO_3 , K_2CO_3), metal-based catalysts (i.e., Ni, Ce, La), and mineral catalysts (i.e., dolomite and olivine), are the most currently used technologies to convert raw biomass materials into combustible gases generally called synthesis gases or syngas [4]. The resulting synthesis gas (syngas) can also be used to produce Fischer-Tropsch fuels, methanol, and oxo alcohols [5]. Syngas normally contains hydrogen (H_2) and carbon monoxide (CO), but often it also contains carbon dioxide (CO_2), methane (CH_4), nitrogen (N_2) and, depending on the feedstock subjected to gasification, a higher or lesser amount of hydrogen sulfide (H_2S), as well as small amounts of other compounds and particles. For example, the percentage of sulfur in the refuse from gardens (green wastes) is 0.18%, in the pine sawdust is 0.57%, in the wood chips is 0.02%, in the wood residue is 0.2%, and in the coffee bean husks is 0.07% [6]. Therefore, the gas resulting from the gasification of these materials will contain different amounts of H_2S . In order to be used in power producing equipment such as gas engines, micro gas turbines, or fuel cells, the syngas must be conditioned in order to meet the required operation conditions [7]. The main syngas contaminants with detrimental effects for such equipment are solid particles, tar, H_2S , HCl, and alkali compounds such as NaOH and KOH [8].

H_2S is known as a toxic odorous gas that causes many technical and environmental problems such as corrosion of equipment, poisoning of catalysts, and formation of acid rain, and therefore its removal from syngas is a priority within gasification plants [9]. In this regard, based on the numerous studies carried out in this field, a wide range of methods for removing H_2S from syngas or other residual gas streams have been identified, tested and applied. Except for the direct conversion of H_2S to sulfur through the Claus process, these methods are conventionally divided into two categories, namely cold gas cleanup (wet and dry) and hot gas cleanup methods. Compared to the first one, the second category has received more attention in recent years due to the advantages it offers, such as avoiding the costs related to cooling the syngas that led to increasing the efficiency of the H_2S removing process, as well as avoiding the generation of waste effluents that require new treatment stages [10]. Therefore, a large assortment of sorbents and catalysis were prepared and tested in different conditions in order to identify the optimum conditions that will ensure the removal of H_2S with the highest efficiency [11–14]. Of these, sorbents based on Zn-Ti were intensively studied due to their proven efficacy for removing H_2S in high temperature operating conditions (i.e., H_2S conversion at 750 °C is close to 100%) [15].

Zinc titanates have been synthesized in different ways (i.e., solid state reaction, polymeric precursor method, hydrothermal method, molten salt method, precipitation method, etc.) and heat treated (calcination) at different temperatures in order to obtain a composite with high physico-chemical stability and adequate reactive and regenerative capacity [16–19]. Generally, the ZnO-TiO₂ binary system may consist of five types of zinc titanates, including ZnTiO_3 (ZnO-TiO₂), Zn_2TiO_4 (2ZnO-TiO₂), and $\text{Zn}_2\text{Ti}_3\text{O}_8$ (2ZnO-3TiO₂), but for high temperature desulfurization of syngas only Zn_2TiO_4 is the most important [20]. However, the end product composition is strongly dependent on the synthesis method and the heat treatment applied [21].

Therefore, the objective of this paper is to investigate through mineralogical, morphological, structural and textural analyzes the influence of calcination temperature on the characteristics of ZnO-TiO₂ composites synthesized through the precipitation method based on micro-sized ZnO and TiO₂ powder mix and ammonium bicarbonate (NH_4HCO_3) solution. The ZnO-TiO₂ composite that exhibited the best characteristics was tested for sulfur removal from a simulated gas stream.

2. Materials and Methods

2.1. Materials

Zinc oxide (ZnO, würtzit form), titanium dioxide (TiO₂, anatase form), and ammonium bicarbonate (NH_4HCO_3) were purchased from Sigma-Aldrich (St. Louis, MO, USA). Ammonium bicarbonate solution of 12.5% (wt.) was freshly prepared by adding a suitable amount of deionized water. Deionized water was used throughout all experiments.

2.2. Composites Synthesis

The ZnO-TiO₂ composites were synthesized through a simple precipitation method which is described in the following. In this respect, ZnO and TiO₂ powders were initially dry mixed at a ZnO:TiO₂ molar ratio of 2:1 for 30 min, after which a solution of ammonium bicarbonate (12.5% NH₄HCO₃) was gradually added for 60 min until a consistent paste was obtained. Next, the paste obtained was vacuum oven dried at 105 °C until a constant mass was reached. The dried paste was pre-calcined at 300 °C for four hours. The obtained product was divided into five samples that were subjected to calcination for four hours at different temperatures. The synthesis conditions are presented in Table 1.

Table 1. Composites synthesis conditions.

Sample Code	ZnO:TiO ₂ Molar Ratio	Preparation Conditions	Calcination Temperature, °C
ZT-300	2:1	Dry mixing of ZnO and TiO ₂ for 30 min	-
ZT-500		Semi-wet mixing of the ZnO and TiO ₂ mixture with ammonium bicarbonate (NH ₄ HCO ₃) solution (12.5% wt.) for 60 min	500
ZT-600		Drying at 105 °C to the constant mass	600
ZT-700		Pre-calcination at 300 °C for 4 h	700
ZT-800		Calcination at different temperatures for 4 h	800

2.3. Composites Characterization

The phase composition analysis of the composites was performed by X-ray diffractometry (XRD) using a model 6000 diffractometer (Shimadzu, Duisburg, Germany; -2θ Bragg-Brentano geometry, using the CuK α characteristic radiations). The elimination of the CuK β component was achieved by a Ni filter. The experimental data were digitally collected through “step by step” scanning method in the 2θ angle interval of 10–90 degrees. Scanning Electron Microscopy (SEM) was performed by using a S2600N scanning electron microscope (Hitachi, Berkshire, United Kingdom). The X-ray qualitative and quantitative microanalyses were performed with an X-ray spectra energy dispersion of Röntec type Brunauer-Emmett-Teller (BET) type. The textural analysis was performed by using an ASAP 2020 physisorption analyzer (Micromeritics, Unterschleissheim, Germany). The samples were first degassed for 2 h at a temperature of 150 °C and pressure of 0.1 Pa and then subjected to analysis. The N₂ adsorption-desorption isotherms of composites were determined at N₂ liquefaction temperature (77.35 K). The surface area was determined from the isotherms data by using Brunauer-Emmett-Teller (BET) method, while the pore size distribution and the pore volume were calculated by using Barrett-Joyner-Halenda (BJH) method. FTIR spectra of composites were recorded with a Tensor 37 instrument (Bruker, Durham, United Kingdom), in attenuated total reflectance mode (ATR, Golden Gate diamond unit). The wavelength range was from 4000 to 400 cm⁻¹ at 64 scans per spectrum, with a resolution of 4 cm⁻¹.

2.4. ZnO-TiO₂ Composite Testing

2.4.1. ZnO-TiO₂ Composite Sulfurization

Two grams of ZnO-TiO₂ composite with a particle size less than 1 mm were sulfurized for five hours by passing a H₂S gas stream through a tubular reactor heated at a temperature of 500 ± 2 °C with a flow rate of 50 mL/min. H₂S was generated by the acid attack (300 mL hydrochloric acid-HCl, 30–35% by mass) of 50 g of iron sulfide (FeS). Prior to sulfurization, the ZnO-TiO₂ composite was activated by passing an argon stream through the tubular reactor heated to 300 °C for 20 min. A sketch of the sulfurization laboratory plant is shown in Figure 1. The installation used for sulfurization is not a standard one. It was developed in-house by the authors.

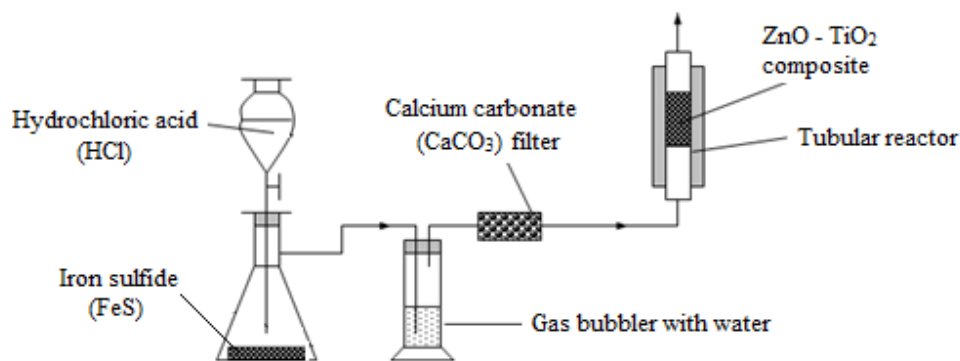


Figure 1. The sketch of the laboratory sulfurization plant.

2.4.2. ZnO-TiO₂ Composite Regeneration

The regeneration of the sulfurized ZnO-TiO₂ composite was carried out by combustion the samples into an oxygen-excess atmosphere. In this respect, 0.2 g of sulfurized ZnO-TiO₂ composite with a particle size less than 1 mm were introduced into an electrically heated oven, preheated at a temperature of 400 °C, which is connected to the gas capture and analysis facility of the formed sulfur dioxide (SO₂). The heating of the oven continues up to a temperature of 950 °C with a rate of 10 °C/min. The sulfur dioxide formed is trapped in an iodine solution (I₂, 0.1 N) added progressively to the bubbling vessel until it has not decolorized anymore. The excess iodine is subsequently titrated with sodium thiosulfate solution (Na₂S₂O₃, 0.1 N) in the presence of starch solution. A sketch of the laboratory plant is shown in Figure 2. The method and the installation used for composite regeneration are not standard. Both of them were developed by us.

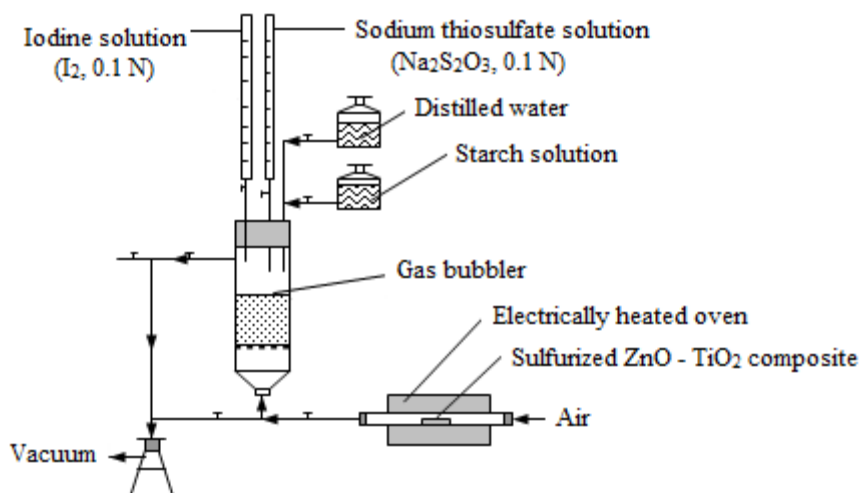


Figure 2. The sketch of the laboratory plant for sulfurized ZnO-TiO₂ composite regeneration.

3. Results and Discussion

3.1. X-Ray Diffractometry

The XRD spectra of the synthesized composites (Figure 3) indicate the significant influence of the temperature at which the heat treatment is carried out. As can be seen, in the low temperature range (300 °C and 500 °C) only ZnO in the wurtzite form (peaks located at $2\theta = 31.82^\circ, 34.471^\circ, 36.309^\circ, 47.592^\circ, 56.647^\circ, 67.996^\circ$, and 69.167° -JCPDS card reference code 01-070-8072) and TiO₂ in the anatase form (peaks located at $2\theta = 25.346^\circ, 37.846^\circ, 48.084^\circ, 53.947^\circ, 55.112^\circ$, and 70.336° -JCPDS card reference code 01-084-1286) as well as in the rutile form (peaks located at $2\theta = 36.302^\circ, 56.647^\circ$, and 62.890° -JCPDS card reference code 01-073-1765) appear in the ZT-300 and ZT-500 composites XRD spectra (Figure 3a,b).

As the temperature rises (600 °C), zinc titanates such as ZnTiO_3 and Zn_2TiO_4 begin to appear in the ZT-600 composite XRD spectrum (Figure 3c). The peaks were attributed to cubic crystallization system of Zn_2TiO_4 located at $2\theta = 29.939^\circ$, 35.217° , 53.0531° , and 56.711° (JCPDS card reference code 01-073-0578), and to rhomboidal crystallization system of ZnTiO_3 located at $2\theta = 32.825^\circ$, 38.771° , 53.015° , 56.844° , 62.907° , and 77.956° (JCPDS card reference code 01-073-0547). At this temperature the unreacted weight percent of ZnO is 53.5% and unreacted weight percent of TiO_2 is 22.2% in anatase form and 10.1% in rutile form. The weight percent of Zn_2TiO_4 formed is 8.1% and the weight percent of ZnTiO_3 formed is 6.1%.

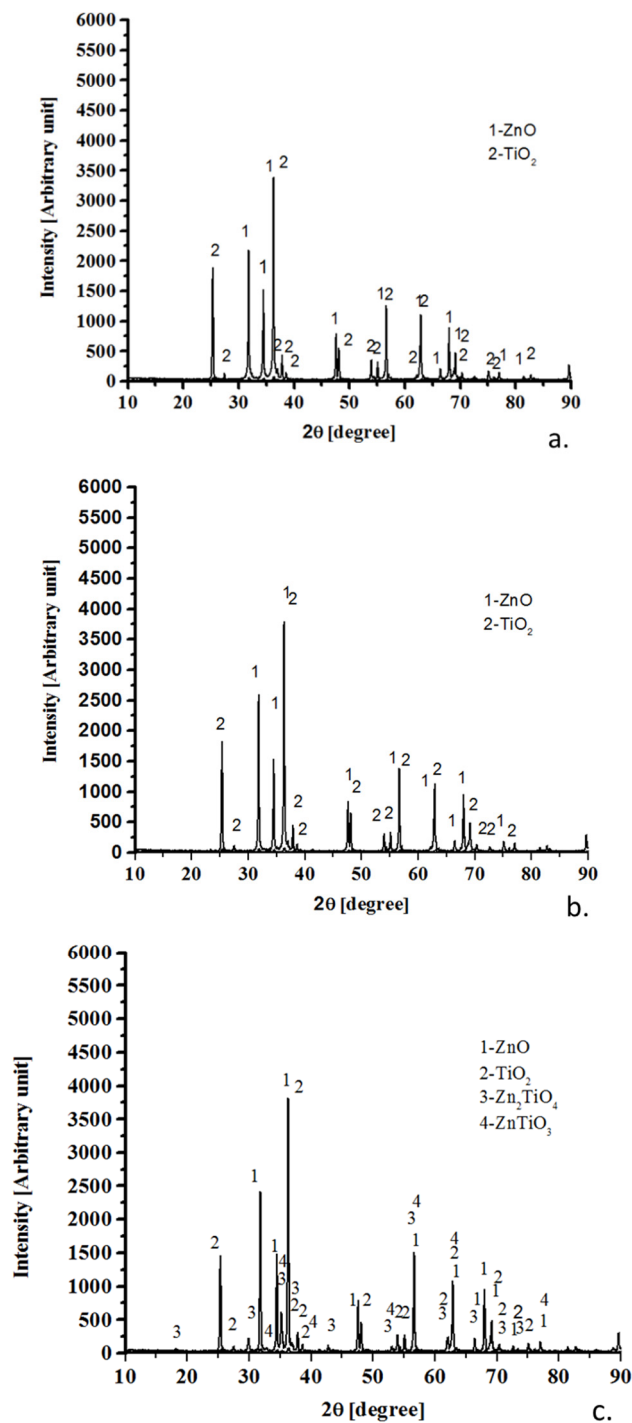


Figure 3. Cont.

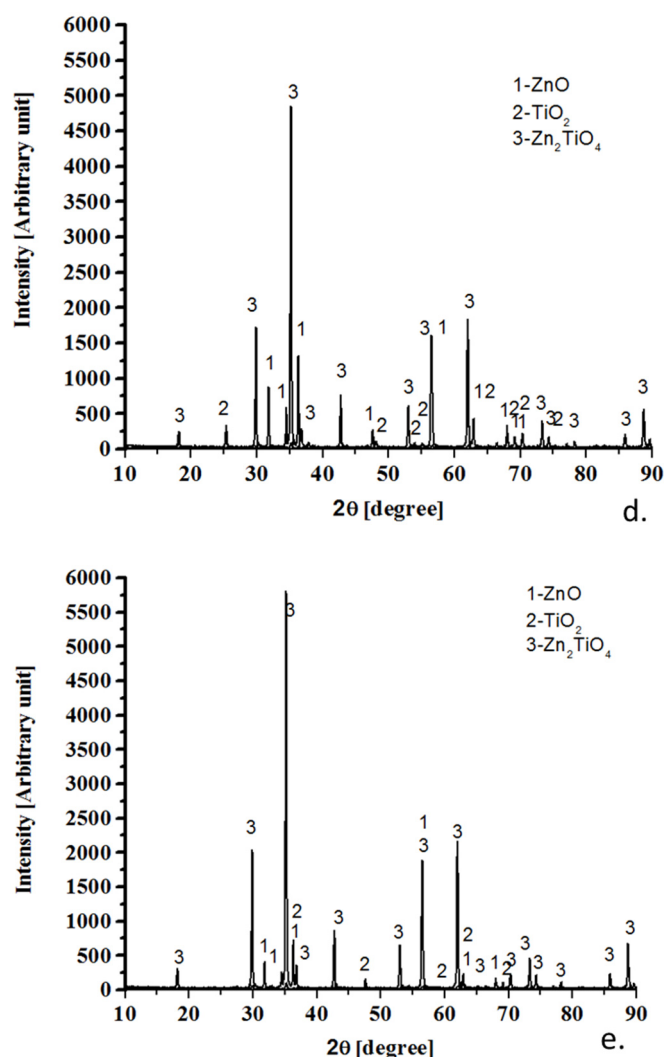


Figure 3. X-ray diffraction (XRD) patterns of synthesized composites: (a) ZT-300, (b) ZT-500, (c) ZT-600, (d) ZT-700, (e) ZT-800.

The spectra of ZT-700 and ZT-800 (Figure 3d,e) show that Zn_2TiO_4 represents the major phase of these synthesized composites (peaks located at $2\theta = 18.161^\circ, 29.939^\circ, 35.217^\circ, 36.387^\circ, 42.627^\circ, 53.053^\circ, 56.641^\circ, 62.933^\circ$, and 73.411° -JCPDS card reference code 01-073-0578). Thus, in the case of ZT-700, the weight percent of Zn_2TiO_4 is 72.7%, and 6.1% TiO_2 (rutile form) and 21.1% ZnO remains unreacted. Regarding ZT-800, the weight percent of Zn_2TiO_4 is 88%, and only 1.8% TiO_2 (rutile form) and 9.8% ZnO remains unreacted. The difference regarding the participation in the reaction of the two oxides components of the ZnO- TiO_2 binary system is that at high calcination temperatures titanium ions (Ti^{4+}) and zinc ions (Zn^{2+}) diffuse at different rates through the zinc oxide layer, the rate of diffusion of titanium ions being greater than that of zinc ions [22,23].

3.2. Infrared Spectroscopy

The FTIR spectra of the synthesized composites are presented in Figure 4. As can be seen, the spectra corresponding to the composites ZT-300, ZT-500, and ZT-600 show a broad absorption band in the range of 3371 to 3381 cm^{-1} , which was attributed to the O-H stretching vibration of the water molecules. This absorption band disappears in the spectra of the composites heat-treated at high temperatures, namely ZT-700 and ZT-800, which is an indicator for the complete dehydration of the ZnO- TiO_2 binary

system. The absorption bands in the frequency intervals of 2318 to 2353 cm^{-1} was associated with the free CO_2 molecule existing in the atmospheric air [20].

Also, the absorption bands (spectra of ZT-300, ZT-500, and ZT-600) in the range of 1409–1411 cm^{-1} and those in the range of 1501–1504 cm^{-1} have been associated with carbonate species which could be derived from the zinc titanate precursors. The peaks located in the range of 722–797 cm^{-1} in the spectra of ZT-300, ZT-500, ZT-600, and ZT-700 are assigned to Ti-O stretching vibration in the octahedral TiO_6 group which is present in TiO_2 , ZnTiO_3 and Zn_2TiO_4 [16,17,24]. It should be noted that, of all these spectra, the one corresponding to the ZT-700 has an adsorption band in this frequency interval with the lowest intensity. However, unlike the others, it presents a new absorption band located at 549 cm^{-1} which was assigned to the same Ti-O stretching vibration which is this time associated with the octahedral TiO_6 group in the Zn_2TiO_4 . The spectrum of ZT-800 has a single absorption band located at approximately the same frequency as in the case of ZT-700 (548 cm^{-1}) spectrum, which is also associated with TiO_6 group in the Zn_2TiO_4 . The peak that appears at 485 cm^{-1} in the spectra of ZT-300, ZT-500, and ZT-600 was assigned to the stretching vibrations of Zn-O bond in ZnO. All these results indicate a progressive transformation of the ZnO-TiO₂ binary system with the increase of the calcination temperature, which becomes predominantly mono-component (i.e., Zn_2TiO_4) at calcination temperatures above 700 °C. These results are consistent with those obtained by XRD analysis.

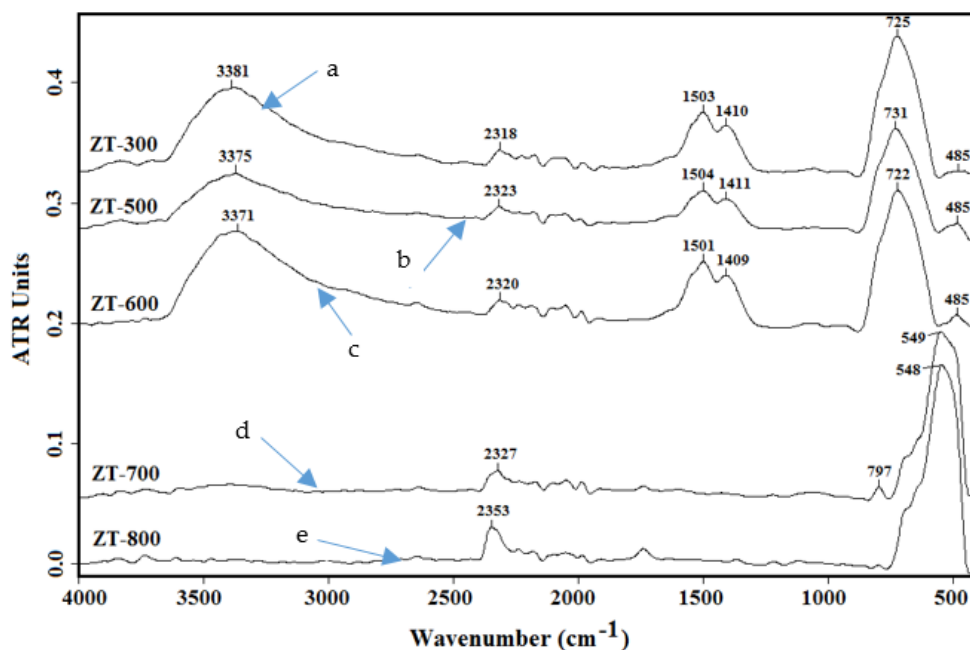


Figure 4. Fourier transform infrared (FT-IR) spectra of synthesized composites: (a) ZT-300, (b) ZT-500, (c) ZT-600, (d) ZT-700, (e) ZT-800.

3.3. Scanning Electron Microscopy

Figure 5 shows the electron micrographs of the synthesized composites. In this respect, the electron micrograph for the sample ZT-300 shows the presence of three types of particles of different sizes. The largest ones, having dimensions ranged between 150–320 nm, were attributed to the ZnO (würtzite form). Smaller particles deposits with the dimensions ranged between 13.4–16.4 nm, which are attributed to the TiO_2 in the anatase form, are grouped on their surface. Small amounts of intermediate-size particles were attributed to the TiO_2 in the rutile form, the dimensions of which vary between 50–75 nm.

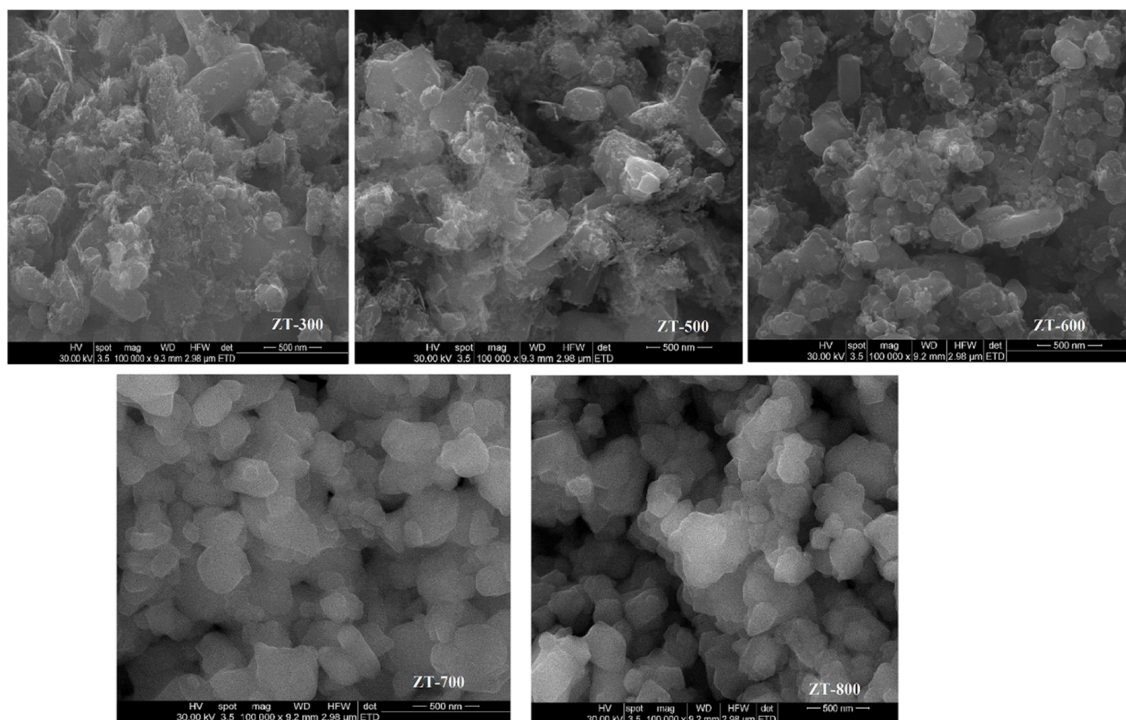


Figure 5. Scanning electron microscope (SEM) images of synthesized composites (100,000× magnification; horizontal field of width HFW = 2.98 μm).

It is also noted that some particles have brighter edges, which suggests their orientation at different heights. The electron micrograph corresponding to the ZT-500 is similar to that of ZT-300 showing large ZnO particles with dimensions ranging between 119–200 nm, TiO₂ particles in anatase form, whose dimensions are small, ranging between 15–22 nm, as well as intermediate-size particles of TiO₂ in the rutile form with dimensions ranged between 80–100 nm. The morphology of ZT-600 begins to look uniform with the dimensions of particles ranging between 18–105 nm. At this calcination temperature, TiO₂ particles in the anatase form get polygonal shapes in comparison with ZT-500 in which the TiO₂ particles do not have a defined form. ZT-700 has a uniform morphology with particles having similar dimensions and regular forms. This morphology suggests the conversion of a large part of TiO₂ and ZnO to zinc titanates, as was also confirmed by XRD results. The particles have a clear outline being in the form of plates stacked one above another with the dimensions ranging between 100–350 nm. Over the calcination temperature of 700 °C zinc titanates particles get sintered and the contours of the particles begin to disappear (electron micrograph of ZT-800). The dimension of particles varies between 110–177 nm.

3.4. Textural Characterization of Synthesized Composites

To characterize the synthesized composites from a textural point of view, a BET analysis of their surfaces was carried out. The adsorption-desorption isotherms as well as the particle size distribution of the synthesized composites are presented in Figure 6.

According to the IUPAC classification [25], the measured adsorption-desorption isotherms of ZT-500 and ZT-600 are of type II (the relative pressure- p/p_0 at which the multilayer adsorption begins is approximately 0.2 for ZT-500 and 0.1 for ZT-600) which indicates that these composites have developed a predominantly non-porous structure with only a limited number of micropores and mesopores.

However, the small type H3 hysteresis that appears on these isotherms indicates some plate-like particles with irregular and slit-shaped pores. The measured adsorption-desorption isotherms of ZT-700 looks rather to be of type III which is also associated with a non-porous material. However, the open hysteresis that appears on the isotherm suggests a small micropore volume developed in this type of

composite with the presence of some very narrow slit pores or bottle shaped pores. A non-homogenous pore size distribution was recorded for all synthesized composites.

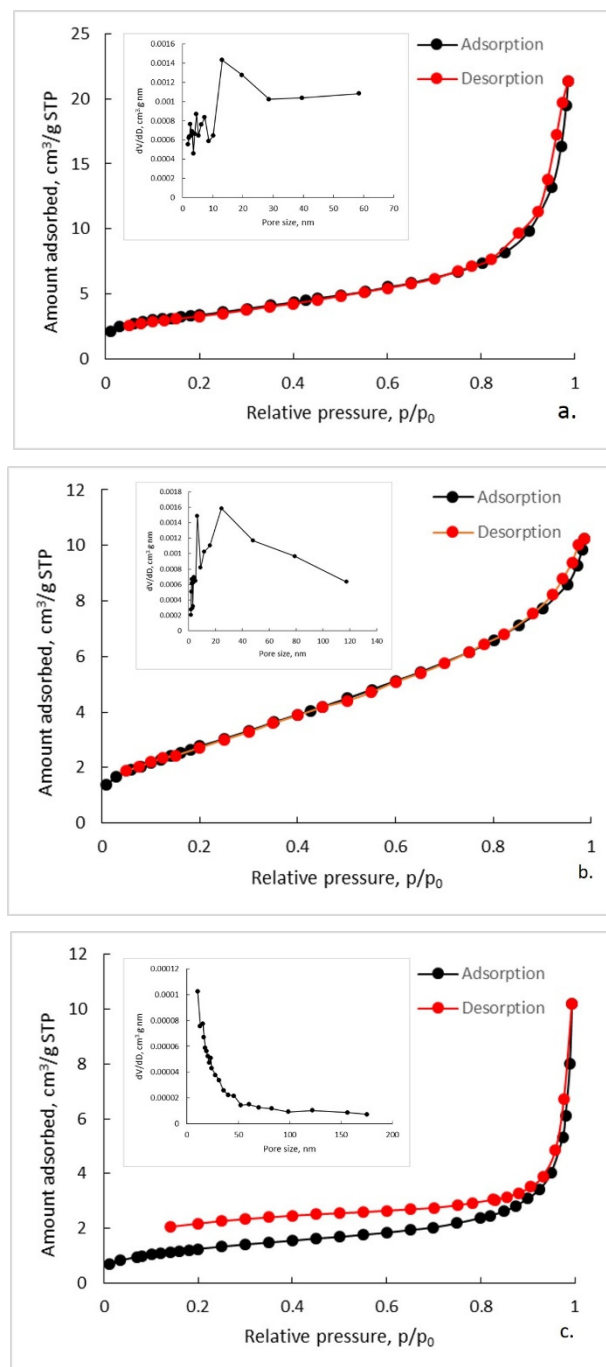


Figure 6. Nitrogen adsorption-desorption isotherms of synthesized composites: (a) ZT-500, (b) ZT-600, (c) ZT-700. Particle size distribution as inset graphs.

Figure 7 shows the variation of BET surface area and pore volume of the synthesized composites according to the calcination temperature. As can be seen, both BET surface area and pore volume decrease with the increasing of calcination temperature. This is most probably due to the increasingly pronounced sintering of the formed zinc titanates, which leads to the closure of the pores [26]. According to the results obtained from the BET analysis, the largest surface area was registered for ZT-500, this being 11.97 m²/g, but as the XRD results have shown, at this calcination temperature the material consists only of Ti and Zn

oxides. With the occurrence of zinc titanates in the system starting with the calcination temperature of 600 °C, the specific surface begins to decrease, so that for ZT-600 this is 10.35 m²/g and for ZT-700 it is only 4.58 m²/g. Similar trend was recorded for pore volume of synthesized composites namely, 0.031 cm³/g for ZT-500, 0.015 cm³/g for ZT-600, and 0.014 cm³/g for ZT-700. This very small pore volume suggests a non-porous-like structure of the synthesized composites [27,28].

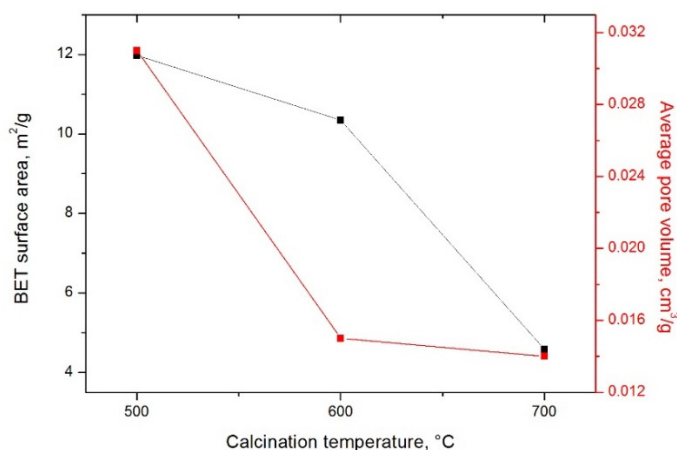


Figure 7. Influence of calcination temperature on the BET surface area and pore volume of the synthesized composites.

3.5. ZnO-TiO₂ Composite Testing

From the mineralogical, morphological, structural and textural analyzes it can be concluded that ZnO-TiO₂ composite obtained by calcination at 700 °C (ZT-700) exhibits the best physicochemical characteristics and, therefore has been tested in respect with its capacity to remove H₂S from a simulated gas stream. The removal degree of sulfur from simulated gas stream obtained with ZT-700 was established from the tests results. The obtained results are presented in Table 2 and Figure 8.

Table 2. Sulfur content and the degree of ZnO consumption in the sample.

Sample Code	ZnO:TiO ₂ Molar Ratio	Theoretical Sulfur Content * (S _t), % (wt.)	Experimental Sulfur Content (S _e), % (wt.)	Sulfur Removal Degree, %
ZT 700	2:1	23.32	22.63	97.04

* The theoretical amount of sulfur is determined by the molar ratio of oxides (ZnO:TiO₂ = 2:1) relative to 100 g of sulfur-saturated mass of sample.

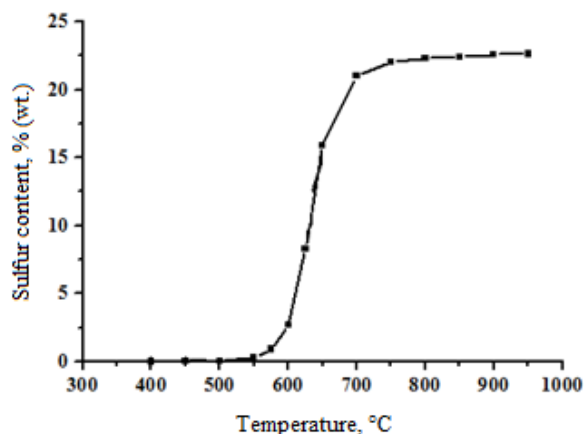
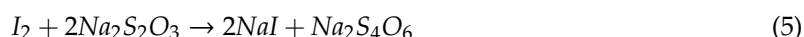


Figure 8. The amount of sulfur removed from the ZT-700 as a function of the calcination temperature.

The equations of the chemical reactions as well as the calculations underlying the experimental determination of the experimental sulfur content in the sample are presented in Equations (1)–(6):



$$S_e = \frac{0.0016 \times (V_1 \times f_1 - V_2 \times f_2)}{m} \times 100 \quad (6)$$

The degree of sulfur removal obtained with ZT-700 was determined with Equation (7):

$$\eta = \frac{S_e}{S_t} \times 100 \quad (7)$$

where S_e is the experimental sulfur content, % (wt.); S_t is the theoretical sulfur content, % (wt.), η is the sulfur removal degree, %; V_1 is the volume of iodine consumed up to the total regeneration of the sulfurized ZT-700, mL; V_2 is the volume of 0.1 N sodium thiosulfate solution used for titration, mL; f_1 is the correction factor of the 0.1 N iodine solution; f_2 is the correction factor of the 0.1 N iodine solution sodium thiosulfate solution; m is the mass of the sulfurized ZT-700 sample, g; 0.0016 is the amount of sulfur (g) corresponding to 1 cm³ of 0.1 N iodine solution.

As it shown in Figure 8, the oxidation of zinc sulfide (ZnS) begins at low temperature values (400–500 °C), and the maximum oxidation rate is reached in the temperature range of 600–700 °C. At these temperatures a content of sulfur of approximate 23% wt. is reached, which corresponds to a maximum sulfur removal degree of approximate 97%. Table 3 presents a comparative study on the efficiency of H₂S removal from syngas between the results obtained in this work and those presented in the literature.

Table 3. Comparative study on the efficiency of H₂S removal from syngas. Values were obtained in the best operation conditions.

Sorbent/Catalyst	Operational Conditions	Removal Efficiency, %	Reference
Dolomite and Ni-based catalyst (Ni 11%, CaO 6–9%, Al ₂ O ₃ 76–82%)	Temperature: 850 °C, atmospheric pressure, saturated conditions	over 97	[29]
G-201 and G-202 sorbents (Zn/Ti molar ratio of 1.5 and 1.0 respectively)	Temperature: 550–650 °C Pressure: 0.8 mpa	over 99	[30]
Non-thermal plasma combined with 5% MoS ₂ /Al ₂ O ₃	Low temperature (120 °C) and atmospheric pressure	98–100	[31]
Zinc oxide	Around 2% humidity and temperature 460 °C	near the 100	[13]
Monolithic sorbent ZTC (Zn:Ti:Co = 1:1:0.25) 60%, natural clay 27%, silica gel 3%, colloidal dispersion of graphite 10%	Temperature: 540 °C	99.6–99.9	[32]
ZT-700 (ZnO:TiO ₂ molar ratio of 2:1; calcinated at 700 °C)	Temperature: 600–700 °C	97	This work

4. Conclusions

The influence of calcination temperature on the characteristics of the ZnO-TiO₂ composites was studied in this work through mineralogical, morphological, structural and textural analysis. From the phase composition standpoint, the results derived from both mineralogical and structural analyzes highlighted that with the increase of calcination temperature the ZnO-TiO₂ system evolves from an exclusively oxide system (calcination temperature of 500 °C) to a composite system consisting mainly of zinc orthotitanate (calcination temperature of 700 °C). The morphological analysis of the synthesized composites showed that as the calcination temperature increases, their component particles undergo a series of dimensional and shape changes that are closely related to the crystalline transformations of the oxide system and to the newly formed zinc titanate types. At high calcination temperatures (700–800 °C) the zinc titanates formed sintering leading to a compact structure of the synthesized composites. The textural analysis revealed the formation of a predominantly non-porous composites, the pore volume and their surface area decreasing with the increasing of calcination temperature.

Therefore, it was found that ZT-700 type composites, which contain predominantly zinc orthotitanate, meets the characteristics that recommend it to be successfully used for the desulfurization of the syngas. In this regard, the tests carried out to establish the sulfur removal capacity of ZT-700 from a simulated gas stream showed that a removal degree of about 97% can be reached, which open the way for further experiments with real syngas. Thus, given the need for power generation using advanced technologies, such as gas/turbine engines or solid fuel cells, it is necessary to reduce the H₂S content to acceptable levels, and the use of ZT-700 type composites is a solution to achieve this objective. Also, in future research, will be pursued a better optimization of ZnO:TiO₂ molar ratio so as to increase the operating performance of these composites and to analyze the possibility of elimination of H₂S and other types of gases.

Author Contributions: Conceptualization, V.P.; Data curation, A.M.D. and C.M.; Formal analysis, C.B.; Funding acquisition, S.C.; Investigation, D.D. and E.V.; Methodology, C.B. and Software, G.G. All authors have read and agreed to the published version of the manuscript.

Funding: This work was supported by the European Regional Development Fund through Competitiveness Operational Program 2014–2020, Priority axis 1, Project No. P_36_611, MySMIS code 107066, Innovative Technologies for Materials Quality Assurance in Health, Energy and Environmental-Center for Innovative Manufacturing Solutions of Smart Biomaterials and Biomedical Surfaces—INOVABIOMED.

Conflicts of Interest: The authors declare no conflict of interest.

References

1. Stolecka, K.; Rusin, A. Analysis of hazards related to syngas production and transport. *Renew. Energy* **2020**, *146*, 2535–2555. [\[CrossRef\]](#)
2. Bassani, A.; Pirola, C.; Maggio, E.; Pettinau, A.; Frau, C.; Bozzano, G.; Pierucci, S.; Ranzi, E.; Manenti, F. Acid Gas to Syngas (AG2S™) technology applied to solid fuel gasification: Cutting H₂S and CO₂ emissions by improving syngas production. *Appl. Energy* **2016**, *184*, 1284–1291. [\[CrossRef\]](#)
3. Motta, I.L.; Miranda, N.T.; Filho, R.M.; Marciel, M.R.W. Biomass gasification in fluidized beds: A review of biomass moisture content and operating pressure effects. *Renew. Sust. Energ. Rev.* **2018**, *94*, 998–1023. [\[CrossRef\]](#)
4. Cao, L.; Yu, I.K.M.; Xiong, X.; Tsang, D.C.W.; Zhang, S.; Clark, J.H.; Hu, C.; Ng, Y.H.; Shang, J.; Ok, Y.S. Biorenewable hydrogen production through biomass gasification: A review and future prospects. *Environ. Res.* **2020**, *186*, 109547. [\[CrossRef\]](#) [\[PubMed\]](#)
5. Wilson, S.M.V.; Tezel, F.H.; Kennedy, D.A. Adsorbent screening for CO₂/CO separation for applications in syngas production. *Sep. Purif. Technol.* **2019**. [\[CrossRef\]](#)
6. Minutillo, M.; Perna, A.; Jannelli, E.; Cigolotti, V.; Nam, S.W.; Yoon, S.P.; Kwon, B.W. Coupling of biomass gasification and SOFC—Gas Turbine Hybrid System for small scale cogeneration applications. *Energy Procedia* **2017**, *105*, 730–737. [\[CrossRef\]](#)

7. Moradi, R.; Marcantonio, V.; Cioccolanti, L.; Bocci, E. Integrating biomass gasification with a steam-injected micro gas turbine and an Organic Rankine Cycle unit for combined heat and power production. *Energy Convers. Manag.* **2020**, *205*, 112464. [\[CrossRef\]](#)
8. Pala, L.P.R.; Wang, Q.; Kolb, G.; Hessel, V. Steam gasification of biomass with subsequent syngas adjustment using shift reaction for syngas production: An Aspen Plus model. *Renew. Energy* **2017**, *101*, 484–492. [\[CrossRef\]](#)
9. Moon, J.; Jo, W.; Jeong, S.; Bang, B.; Choi, Y.; Hwang, J.; Lee, U. Gas cleaning with molten tin for hydrogen sulfide and tar in producer gas generated from biomass gasification. *Fuel* **2017**, *130*, 318–326. [\[CrossRef\]](#)
10. Abdoulmoumine, N.; Adhikari, S.; Kulkarni, A.; Chattanathan, S. A review on biomass gasification syngas cleanup. *Appl. Energy* **2015**, *155*, 294–307. [\[CrossRef\]](#)
11. Cecilia, J.A.; Soriano, M.D.; Natoli, A.; Rodríguez-Castellón, E.; Nieto, J.M.L. Selective oxidation of hydrogen sulfide to sulfur using vanadium oxide supported on porous clay heterostructures (PCHs) formed by pillars silica, silica-zirconia or silica-titania. *Materials* **2018**, *11*, 1562. [\[CrossRef\]](#) [\[PubMed\]](#)
12. Frilund, C.; Simell, P.; Kaisalo, N.; Kurkela, E.; Koskinen-Soivi, M.-L. Desulfurization of biomass syngas using ZnO-based adsorbents: Long-term hydrogen sulfide breakthrough experiments. *Energ. Fuel* **2020**. [\[CrossRef\]](#) [\[PubMed\]](#)
13. Marcantonio, V.; Bocci, E.; Ouweltjes, J.P.; Zotto, L.D.; Monarca, D. Evaluation of sorbents for high temperature removal of tars, hydrogen sulphide, hydrogen chloride and ammonia from biomass-derived syngas by using Aspen Plus. *Int. J. Hydrogen Energy* **2020**, *45*, 6651–6662. [\[CrossRef\]](#)
14. Kailasa, S.K.; Koduru, J.R.; Vikrant, K.; Tsang, Y.F.; Singhal, R.K.; Hussain, C.M.; Kim, K.-H. Recent progress on solution and materials chemistry for the removal of hydrogen sulfide from various gas plants. *J. Mol. Liq.* **2020**, *297*, 111886. [\[CrossRef\]](#)
15. Tuna, Ö.; Simsek, E.B.; Sarioğlu, A.; DurakÇetin, Y. Influence of the process conditions on the kinetic behaviour of zinc orthotitanate for syngas clean-up. *Biomass Bioenerg.* **2019**, *128*, 105326. [\[CrossRef\]](#)
16. Macedo, K.R.M.; Oliveira, G.A.C.; Pereira, K.A.B.; Mendes, L.C.; Araújo, A.S.; Cassella, R.J. Titanium-zinc polycitrate precursor: Influence of thermal treatment on structural, thermal, optical characteristics of zinc titanates. *Mater. Chem. Phys.* **2019**, *236*, 121768. [\[CrossRef\]](#)
17. Budigi, L.; Nasina, M.R.; Shaik, K.; Amaravadi, S. Structural and optical properties of zinc titanates synthesized by precipitation method. *J. Chem. Sci.* **2015**, *127*, 509–518. [\[CrossRef\]](#)
18. Untea, I.; Dancila, M.; Vasile, E.; Belcu, M. Structural, morphological and textural modifications of ZnO–TiO₂ HTGD based sorbents induced by Al₂O₃ addition, thermal treatment and sulfurizing process. *Powder Technol.* **2009**, *191*, 27–33. [\[CrossRef\]](#)
19. Kubiak, A.; Siwińska-Ciesielczyk, K.; Jesionowski, T. Titania-based hybrid materials with ZnO, ZrO₂ and MoS₂: A review. *Materials* **2018**, *11*, 2295. [\[CrossRef\]](#)
20. Ayed, S.; Abdelkefi, H.; Khemakhem, H.; Matoussi, A. Solid state synthesis and structural characterization of zinc titanates. *J. Alloys Compd.* **2016**, *677*, 185–189. [\[CrossRef\]](#)
21. Chaves, A.C.; Lima, S.J.G.; Araújo, R.C.M.U.; Maurera, M.A.M.A.; Longo, E.; Pizani, P.S.; Simões, L.G.P.; Soledade, L.E.B.; Souza, A.G.; dos Santos, I.M.G. Photoluminescence in disordered Zn₂TiO₄. *J. Solid State Chem.* **2006**, *179*, 985–992. [\[CrossRef\]](#)
22. Arin, J.; Thongtem, S.; Phuruangrat, A.; Thongtem, T. Template synthesis of Zn₂TiO₄ and Zn₂Ti₃O₈ nanorods by hydrothermal calcination combined processes. *Mater. Lett.* **2017**, *193*, 270–273. [\[CrossRef\]](#)
23. Fu, L.; Zhu, J.; Huang, W.; Fang, J.; Sun, X.; Wang, X.; Liao, K. Preparation of Nano-Porous Carbon-Silica Composites and Its Adsorption Capacity to Volatile Organic Compounds. *Processes* **2020**, *8*, 372. [\[CrossRef\]](#)
24. Chai, Y.-L.; Chang, Y.-S.; Chen, G.-J.; Hsiao, Y.-J. The effects of heat-treatment on the structure evolution and crystallinity of ZnTiO₃ nano-crystals prepared by Pechini process. *Mater. Res. Bull.* **2008**, *43*, 1066–1073. [\[CrossRef\]](#)
25. Li, X.; Huang, W.; Liu, X.; Bian, H. Graphene oxide assisted ZIF-90 composites with enhanced n-hexane vapor adsorption capacity, efficiency and rate. *J. Solid State Chem.* **2019**, *278*, 120–890. [\[CrossRef\]](#)
26. Brito, L.; Almenglo, F.; Martín Ramírez, M.; Cantero, D. Feedback and Feedforward Control of a Biotrickling Filter for H₂S Desulfurization with Nitrite as Electron Acceptor. *Appl. Sci.* **2019**, *9*, 2669. [\[CrossRef\]](#)
27. Kubiak, A.; Siwińska-Ciesielczyk, K.; Bielan, Z.; Zielińska-Jurek, A.; Jesionowski, T. Synthesis of highly crystalline photocatalysts based on TiO₂ and ZnO for the degradation of organic impurities under visible-light irradiation. *Adsorption* **2019**, *25*, 309–325. [\[CrossRef\]](#)

28. Nethi, S.K.; Anand, P.N.A.; Rico-Oller, B.; Rodríguez-Diéguez, A.; Gómez-Ruiz, S.; Patra, C.R. Design, synthesis and characterization of doped-titanium oxide nanomaterials with environmental and angiogenic applications. *Sci. Total Environ.* **2017**, *599–600*, 1263–1274. [[CrossRef](#)]
29. Pinto, F.; André, R.N.; Franco, C.; Lopes, H.; Carolino, C.; Costa, R.; Gulyurtlu, I. Co-gasification of coal and wastes in a pilot-scale installation. 2: Effect of catalysts in syngas treatment to achieve sulphur and nitrogen compounds abatement. *Fuel* **2010**, *89*, 3340–3351. [[CrossRef](#)]
30. Bu, X.; Ying, Y.; Ji, X.; Zhang, C.; Peng, W. New development of zinc-based sorbents for hot gas desulfurization. *Fuel Process. Technol.* **2007**, *88*, 143–147. [[CrossRef](#)]
31. Zhang, L.; Liu, X.; Mu, X.; Li, Y.; Fang, K. Highly selective conversion of H_2S-CO_2 to syngas by combination of nonthermal plasma and MoS_2/Al_2O_3 . *J. CO₂ Util.* **2020**, *37*, 45–54.
32. Chomiak, M.; Trawczyński, J.; Blok, Z.; Babiński, P. Monolithic Zn–Co–Ti based sorbents for hot syngas desulfurization. *Fuel Process. Technol.* **2016**, *144*, 64–70. [[CrossRef](#)]



© 2020 by the authors. Licensee MDPI, Basel, Switzerland. This article is an open access article distributed under the terms and conditions of the Creative Commons Attribution (CC BY) license (<http://creativecommons.org/licenses/by/4.0/>).